

# Development of Alumina Investment Shell Molds to Cast 7075 Al-Alloy

A. Chennakesava Reddy

Associate Professor, Department of Mechanical Engineering  
Vasavi College of Engineering, Hyderabad, India

**Abstract:** The ceramic shells were fabricated with ceramic slurry containing alpha and gamma alumina as filler materials and colloidal silica binder. The shell characteristics in terms of bending strength and thermal expansion were measured. The phase transformation from gamma to alpha alumina were observed with transmission electron microscopy (TEM) and selected area electron diffraction (SAED) patterns. The metal to mould reaction were revealed with optical microstructures and hardness distribution. The bonding mechanism in the alumina and colloidal silica binder system was due to formation siloxane bonds. The phase transition  $\gamma \rightarrow \alpha\text{-Al}_2\text{O}_3$  occurs in two phases, respectively in the temperature ranges of 600°C - 850°C cubic crystal structure and from 850°C - 1000°C,  $\alpha\text{-Al}_2\text{O}_3$  with corundum crystal structure. The cracks have been observed in the investment shells made of gamma alumina after 7075 Al-alloy pouring.

**Keywords:** Investment shells, alpha alumina, gamma alumina, bonding mechanism, thermal shock, metal-mould reaction, 7075 Al-alloy.

## 1. Introduction

7075 are often used in transport applications, including marine, automotive and aviation, due to their high strength-to-density ratio. One interesting use for 7075 is in the manufacture of M16 rifles for the American military. In particular high quality M16 rifle lower and upper receivers as well as extension tubes are made from 7075-T6 alloy [1].  $\text{Al}_2\text{O}_3$  is a chemical compound of aluminum and oxygen. It is an electrical insulator but has a relatively high thermal conductivity for a ceramic material. The materials used to build the investment shell moulds, especially refractories, play a vital role in the production of quality castings [2-6]. The properties of refractory fillers, which affect the shell quality, are melting point, thermal expansion, and metal - mould interaction. During the casting process, molten zirconium alloys can easily react with the mold materials and produce a surface contamination layer.

In the present work, alumina was used as refractory filler material to fabricate investment shell moulds for casting of magnesium alloy AZ91E alloys.

## 2. Materials and Methods

The colloidal silica binder was used to fabricate the ceramic shells from alumina ( $\text{Al}_2\text{O}_3$ ) as a reinforced filler material. The specifications of colloidal silica binder is given in table 1. Two grades (primary and backup sands) of stuccoing sand were employed in the present investigation. Finer grade silica sand having AFS grain fineness number 120 was employed for primary coats. This is synthetic sand. This sand was used for first two coats, called prime coats to get good surface finish and every detail of the wax pattern. Coarser grade sand having AFS grain fineness number 42 was employed for back

up coats. This is river sand. The backup sand was employed to develop more thickness to the shell walls with minimum coats.

Table 1. Specifications of silox binder

Property	Amount
Silica ( $\text{SiO}_2$ ) Wt%	30
$\text{pH}$ at 25°C	10.5
Titration Alkali ( $\text{Na}_2\text{O}$ )	0.6
Chlorides/ Sulphates	Traces
Specific gravity, g/cc	1.23

### 2.1 Manufacture of ceramic shells and 7075 alloy castings

The preparation of investment slurry is shown in figure 1. Dip coating slurries were prepared by adding the refractory filler powder to the binder liquid, using sufficient agitation to break up agglomerates and thoroughly wet and disperse the powder. The filler/binder ratio in the slurry was according to the design of experiments. The fabrication of investment shells and casting of 7075 aluminum alloy is shown in figure 2. The investment shells were made of applying a series of ceramic coatings to the wax patterns. The pattern was first dipped into the dip-coating slurry bath. The pattern drains off excess magnesia slurry and to produce a uniform layer. The wet layer was immediately stuccoed with coarse silica sand. Each coating was allowed to dry in the open air. The operations of coating, stuccoing, and drying were repeated six times. The seventh coat was left unstuccoed to avoid the occurrence of loose particles on the shell surface. The first two coats were stuccoed with sand of AFS fineness number 120 and the next four coats were with sand of AFS fineness number 42. After all coats, the shells were air dried for 24 hours. Two shells of each treatment were made.

The 7075 aluminum alloy was melted in an oil fired furnace. During melting, the alloy was coated with flux (covral-11S)

to prevent the oxidation of the metal. The liquid metal was degasified with tetrachloroethane tablets and also modified with sodium. The liquid alloy was gravity poured into the pre-heated ceramic shells. The shells were knocked off by hand hammer after solidification of the molten. The castings were cleaned with soft brush and visually inspected for pins and projections.



Figure 1. Preparation of investment slurry



Figure 2. Fabrication investments shells and casting of 7075 aluminum alloy.

**2.2 Hot strength of ceramic shells**

The dimensions of specimens are 25mm X 32mm X *t* mm, where *t* is the thickness of the shell. The specimens used for bending test are shown in figure 3. The test of hot modulus of rupture was conducted on the universal sand- strength testing machine.

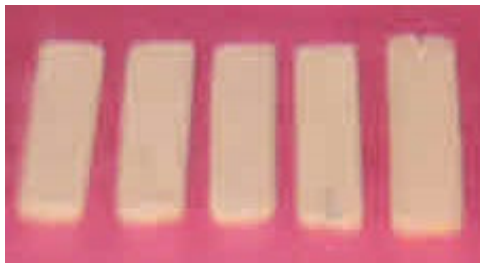


Figure 3. Specimens for bending tests

**2.3 % thermal expansion of ceramic shells**

It was measured in terms of %volume expansion of the investment shells [9]. The length, width and thickness of the shells were measured using vernier calipers before and after sintering in the electrical oven. The % thermal expansion was computed using the following formula:

$$\% \text{ thermal expansion} = \frac{V_2 - V_1}{V_1} \times 100$$

where,  $V_1$  is the volume of the shell before sintering and  $V_2$  is the volume of the shell after sintering.

**3. Results and Discussion**

Kappa alumina has an orthorhombic crystal structure (figure 4a). Gamma alumina is cubic (figure 4b). Alpha alumina is the only stable alumina phase at all temperatures (figure 4c). It has a trigonal structure. In the present work, gamma and alpha alumina particles (figure 5) were used.

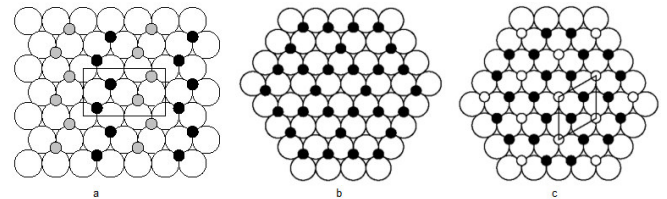


Figure 4. Schematic diagram of first layer Alumina structure: (a) Kappa, (b) Gamma and (c) Alpha.

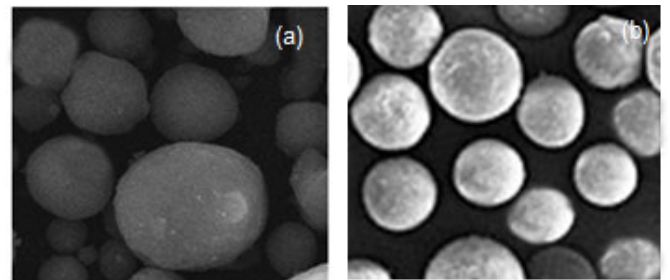


Figure 5. Scanning electron micrograph of (a) gamma and (b) alpha alumina particles.

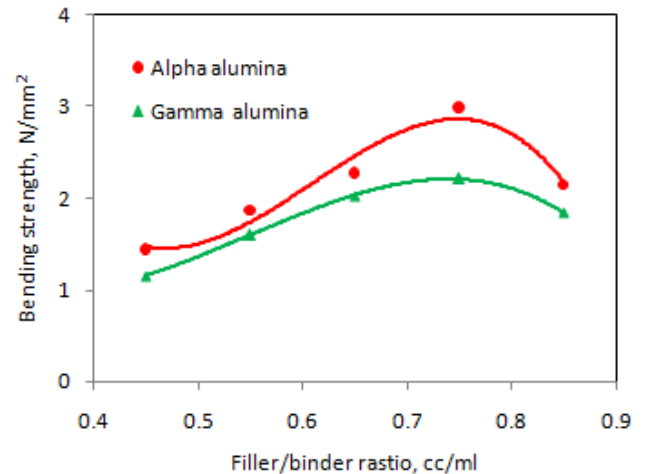


Figure 6. Effect of filler/binder ratio on bending strength.

**3.1 Bonding mechanism in investment shells**

The effect of filler/binder ration on the bending strength of alumina investment shells is shown in figure 6. The bending strength alumina investments shells was found to be high for filler/binder ratio of 0.75 cc/ml. The alpha alumina has greater bonding strength than that of the gamma alumina investment shells. The bonding mechanism in the alumina investment shells is shown in figure 7. Colloidal silica

binder is stable water-based suspension (figure 7a), containing up to 30 wt% of nanometric spherical amorphous silica particles (8-15 nm diameter). When combined with alumina solid particles (figure 7b), colloidal silica can be linked together in branched chains, in a process known as gelation [7, 8], which can be induced by water removal. During the drying step, the hydroxyl groups (Si-OH) on the surface of the particles generate siloxane bonds (Si-O-Si), which results in a three-dimensional network (figure 7c). The micro silica-around colloidal silica system presents a pH value around 4-6, which is closer to the pH where the colloidal silica gelling rate is maximum (around pH 5).

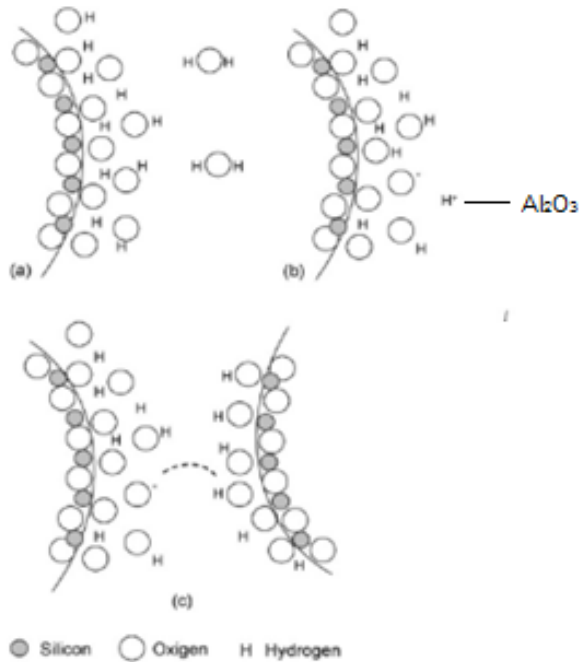


Figure 7. Bonding mechanism in investment shells.

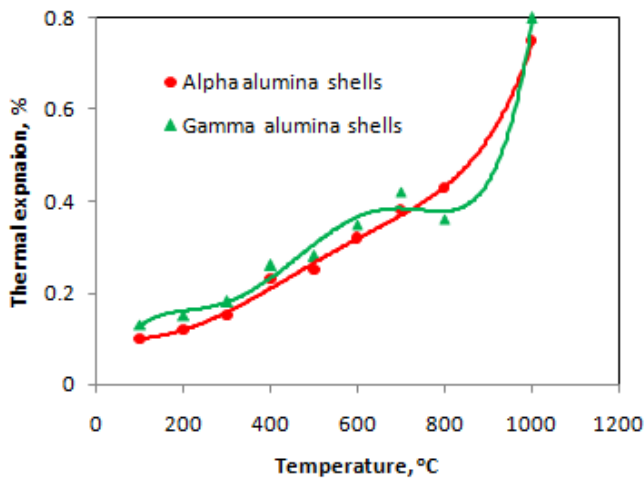


Figure 8. Effect of temperature on thermal expansion of shells.

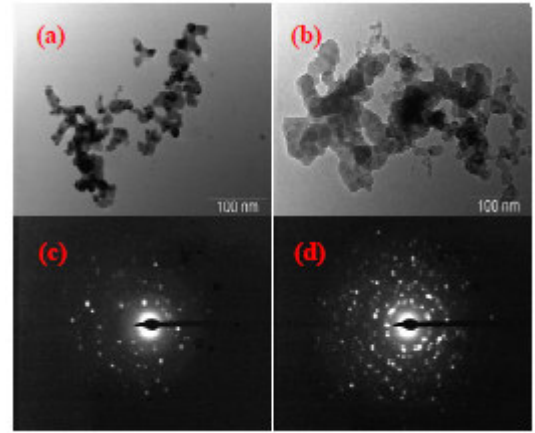


Figure 9. TEM, SAED patterns micrographs of alumina powders at temperatures: (a) and (c) at 800°C and (b) and (d) at 1000°C.

### 3.2 Thermal shock in investment shells

The thermal expansion curve for investment shells is illustrated in figure 8. In case alpha alumina investment shells the thermal expansion was stable and it increased with increase of temperature. The fluctuation in thermal expansion curve of gamma alumina investment shells was on account of phase transition of gamma alumina into alpha alumina at high temperatures around 800°C.

As observed from transmission electron microscopy (TEM) and selected area electron diffraction (SAED) patterns, the phase transition  $\gamma \rightarrow \alpha\text{-Al}_2\text{O}_3$  occurs in two phases (figure 9). The first phase, in the temperature range from 600°C - 850°C, constituted of  $\gamma\text{-Al}_2\text{O}_3$  with cubic crystal structure. In the second phase, in the temperature range from 850°C - 1000°C,  $\alpha\text{-Al}_2\text{O}_3$  with corundum crystal structure. The cracks due to thermal were clearly observed in the cast shells of gamma alumina (figure 10b) where as no cracks were noticed in the alpha alumina shells. This is in agreement with nature of thermal expansion of alumina investment shells.

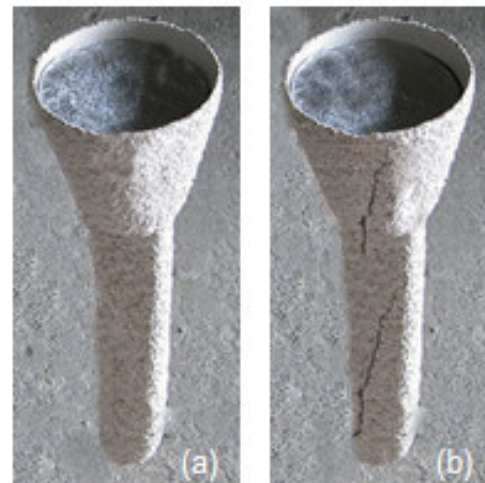


Figure 10. Thermal shock in the investment shells (a) alpha alumina and (b) gamma alumina.

### 3.3 Metal-shell reaction

Figure 11 shows the hardness profile of a sample from 25mm thick 7075 Al-alloy castings made in alumina investment shell molds. The hardness has a function of depth from the surface decrease with an increase in depth. The hardness profile was nearly same in the castings made in alpha and gamma alumina investment shells (figure 12). Fine grain structure was revealed at the metal-mould interface as the general phenomena of beginning of nucleation at the metal-mould interface (figure 12 b). Formation of intermetallic phases (figure 12d) was observed from the microstructure cited at metal-mould interface. The metal-mould reactions were also confirmed from EDX graph shown in figure 12c.

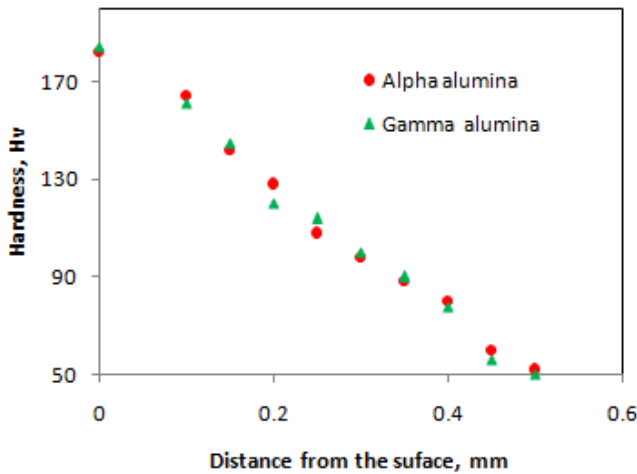


Figure 11. Harness distribution across cross-section of 7075 Al-alloy specimens.

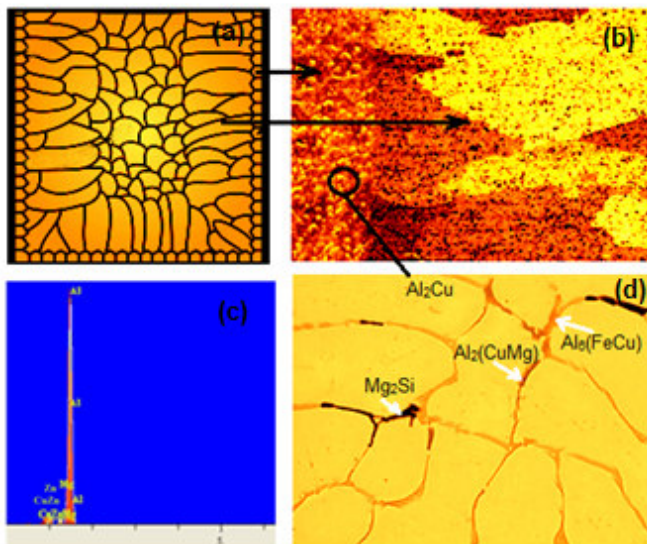


Figure 12. Metal-mould reaction (a) schematic representation grain formation in shell mould, (b) fine grain structure as metal-mould interface (c) EDX graph representing metal-mould reactions and (d) formation of intermetallic phases due to metal-mould reactions

### 4. Conclusions

The bonding mechanism in the alumina and colloidal silica binder system is due to formation siloxane bonds. The phase transition  $\gamma \rightarrow \alpha\text{-Al}_2\text{O}_3$  occurs in two phases, respectively in the temperature ranges of  $600^\circ\text{C} - 850^\circ\text{C}$  cubic crystal structure and from  $850^\circ\text{C} - 1000^\circ\text{C}$ ,  $\alpha\text{-Al}_2\text{O}_3$  with corundum crystal structure. The cracks have been observed in the investment shells made of gamma alumina after 7075 Al-alloy pouring. Intermetallic compounds have been formed due to metal-mould reactions.

### References

1. Alcoa 7075 data sheet.
2. A. Chennakesava Reddy, H.B. Niranjan and A.R.V. Murti, Optimization of investment shell mould using colloidal silica binder, Indian Journal of Engineering & Materials Sciences, vol.3, no.5, pp. 180-184, 1996.
3. A. Chennakesava Reddy and V.S.R. Murti, Studies on Lost-wax process using silox binder, X-ISME Conference on Mechanical Engineering, New Delhi, December, 1996.
4. A. Chennakesava Reddy, V.S.R.Murthi and S. Sundararajan, Regression modelling approach for the analysis of investment shell moulds from coal-flyash, Foundry Magazine, vol. 9, no.5, pp. 36-40, 1997.
5. S. Madhav Reddy and A. Chennakesava Reddy, Interfacial Reaction between Magnesium Alloy and magnesia Ceramic Shell Mold, National Conference on Advanced Materials and Manufacturing Technologies, Hyderabad, 18-20 March 2000.
6. A. Chennakesava Reddy, V.S.R.Murthi and P.M.Jebaraj, A new technique for measurement of the strength of ceramic shells in the precision casting process, Journal of Testing and Evaluation, vol. 28, no.3, pp. 224-226, 2000.
7. A. Chennakesava Reddy, Characterization of ceramic shells fabricated using yttria as reinforcing filler, National Conference on Advanced Materials and Manufacturing Technologies, Hyderabad, December, 1997.
8. A. Chennakesava Reddy, S. Sundararajan, Characterization of ceramic shells using rutile (titania) as reinforcing filler at casting temperature, National Conference on Advanced Materials and Manufacturing Technologies, Hyderabad, December, 1997.
9. N.A. Luneva, Coefficient of thermal expansion of investment moulds, Sov. Cast. Technol. No.1, p.36, 1987.